IJCRT.ORG ISSN : 2320-2882

INTERNATIONAL JOURNAL OF CREATIVE RESEARCH THOUGHTS (IJCRT)

An International Open Access, Peer-reviewed, Refereed Journal

Quantum Computational And Spectroscopic Studies (FT-IR, FT-Raman, NMR And UV-Vis) On Uracil-5-Secondary Sulfonamides

B. Ramachandra[1] Y. Kiran Kumar[2] G.V.Gaurav[3] CH Giridhar[4]

[1]Departments of Chemistry, Basic Sciences and Humanities, Annamacharya Institute of Technology and Sciences, Tirupati-517520, A.P, India.

[2]Departments of Chemistry, Ramireddy Subbarami Reddy Engineering college, Kadanuthala, SPSR Nellore dt, Andhra Pradesh, Pin 524201.

[3]Department of Chemistry, Anil Neerukonda Institute of Technology and Sciences, Sangivalasa, Visakhapatnam 531162, A.P, India

[4]Mallareddy Engineering college, Maisammaguda, Medchel TG,India.

ABSTRACT: Uracil and its derivatives are considered as a revolutionary discovery in the development of drugs, due to their broad spectrum of antiviral and anti-tumour properties. Hence, investigating the molecular characteristics of uracil including its related compounds is essential. In this study, computational quantum chemical (CQC), Pharmacokinetic and biological characteristics have been computed for Uracil-5-Secondary Sulfonamides. These molecules have been extensively characterized using FT-IR, FT-Raman, NMR (^{13}C ^{1}H) and UV-Vis spectroscopic methods by means of empirical as well as computational analysis. Density functional Theory (DFT) assessments were executed utilizing "B3LYP/6--31+ G (d, p) & B3LYP/6--311+ G (2d, p)" component patterns in order to get the molecules' appropriate geometrical attributes. Gauge-independent atomic orbital (GIAO) method it was utilized to ascertain whether the chemical shifts in NMR and UV-Vis spectra. Hyperpolarizabilities, energy diagrams for Computed were the lowest unoccupied molecular orbitals (LUMO) and highest occupied molecular orbitals (HOMO). In addition, Pharmacokinetic properties (ADME/T), drug likeness, bioactivity score, logP, dissociation constant have been computed using Molinspiration, Swiss ADME, Chem Axon and pkCSM.

Key Words: Quantum Computational, Spectroscopic, FT-IR, FT-Raman, NMR and UV-Vis

1. INTRODUCTION

In the field of pharmaceutical development, uracil is regarded as desirable materials due to their diverse biological functions and synthetic affordability. Uracil and its derivatives exhibit a broad array of antiviral and anti-tumour activities. In particular, 5-Fluorouracil (5-FU) is an antimetabolite employed for the therapy of liver, breast, and tumors in the stomach. [1]. The nucleoside compounds of 5- iodouracil and 5-trifluoromethyluracil which are N1-substituted derivatives show antiviral activity while N1, N3-disubstituted uracils exhibit antibacterial and antifungal activities. Hence, exploring the molecular features of N-substituted Uracil-5-Secondary Sulfonamides will be very beneficial in anticancer drug discovery applications. Hence, the present work deals with the computational quantum chemical studies, pharmacokinetics, and other physico-chemical aspects of "N-cyclobutyl-2,4-dioxo-1,2,3,4-tetrahydropyrimidine-5-sulfonamide" (Molecule1) and "N-(1-methoxyethyl)-2,4-dioxo-1,2,3,4 tetrahydropyrimidine-5-sulfonamide" (Molecule 2). The synthesis, characterization, and activity studies of these molecules have been reported earlier by our group.

2. MATERIALS AND METHODS

Parameters of assessment

The chemical predictions have been performed practically utilizing Gaussian 16 software package [2]. Effectiveness of geometrical aspects of compound 1 and compound 2 have been carried out with " B3LYP - Becke, 3-parameter, Lee-Yang–Parr" exchange correlation functional with "6--31+G (d, p), 6--311+G (2d, p)" basis sets. The Gauss View 6 program [3] was used for visualisation when the Gaussian 16 software package is used. The theoretical NMR (^{1}H and ^{13}C) chemical shifts were obtained at "B3LYP/6--31+G (d, p), B3LYP/6--311+G (2d, p)" theoretical level, utilizing the GIAO technique, while the Dimethyl sulfoxide (DMSO) It was perceived as the accepted testimonial. Using Time Dependent-Density Functional theory "CAM-B3LYP/6--311+G (2d, p)" basis set, hypothetical wavelength of the absorption (λ), oscillators intensities (f) and significant involvement to the electronic shifts had been chosen in DMSO as solvent (SMD model). Biological aspects like Molinspiration was used to measure therapeutic similarity, the field of pharmaceutical lipophilicity, detoxification, metabolism, and absorption, shipment, and hazard likeness were carried out by using Molinspiration [4,5], pkCSM[6], SwissADME[7,8] and Chemaxon[9] tools.

3. RESULTS AND DISCUSSION

3.1. Optimized Geometry

The optimized geometrical properties of both the compounds have been computed by "DFT/B3LYP 6--31+G (d, p), DFT/B3LYP 6--311+G (2d, p)" level of theory. Figures 1 and 2 display the submitted and enhanced configurations with atom markings. Both the solvent stage and the gaseous state were studied throughout the present research Investigations were carried out in both gas and liquid phases. Infrared, ^{1}H and ^{13}C NMR results obtained in DFT calculations have been compared with the experimental results of sasidhar. [B Venkata Sasidhar, Ph.D. thesis, GITAM (Deemed to be University), 2015].

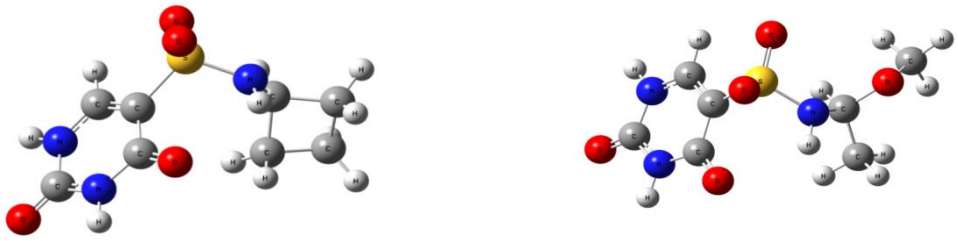

Fig.1: Input structure of"N-cyclobutyl-2,4-dioxo-1,2,3,4-tetrahydropyrimidine-5-sulfonamide" and "N-(1-methoxyethyl)-2,4-dioxo-1,2,3,4-tetrahydropyrimidine-5-sulfonamide"

Fig. 2: The optimized geometrical structure of "N-cyclobutyl-2,4-dioxo-1,2,3,4-tetrahydropyrimidine-5-sulfonamide"and**"**N-(1-methoxyethyl)-2,4-dioxo-1,2,3,4-tetrahydropyrimidine-5-sulfonamide" in solvent phase

3.2 Vibrational Spectral Analysis

The experimental FT-IR spectra (Sasidhar, 2016) were compared to the vibration spectra computed from computational chemical studies. The compounds 1 and 2 consist of 27 atoms and 128 electrons, 27 atoms and 130 electrons. The Fig. The proposed and actual FT-IR spectra of the two substances are presented in figures 3 and 4, correspondingly. The experimental (FT-IR) measurements, calculated vibrational wave numbers, complete fundamental vibrational modes are presented in Table 1 and 2. Due to electron effects of correlation and insufficient foundation sets, the measured wave counts are usually smaller than the calculated wave numbers. As a consequence, the number of waves is obtained and normalized having the scaling factor of 0.933. The results are summarized. The spectrum that was produced can be seen in Figures 5 and 6. Using Raman scattering intensities (Si) are computed using the GAUSSIAN 16 method of calculations.

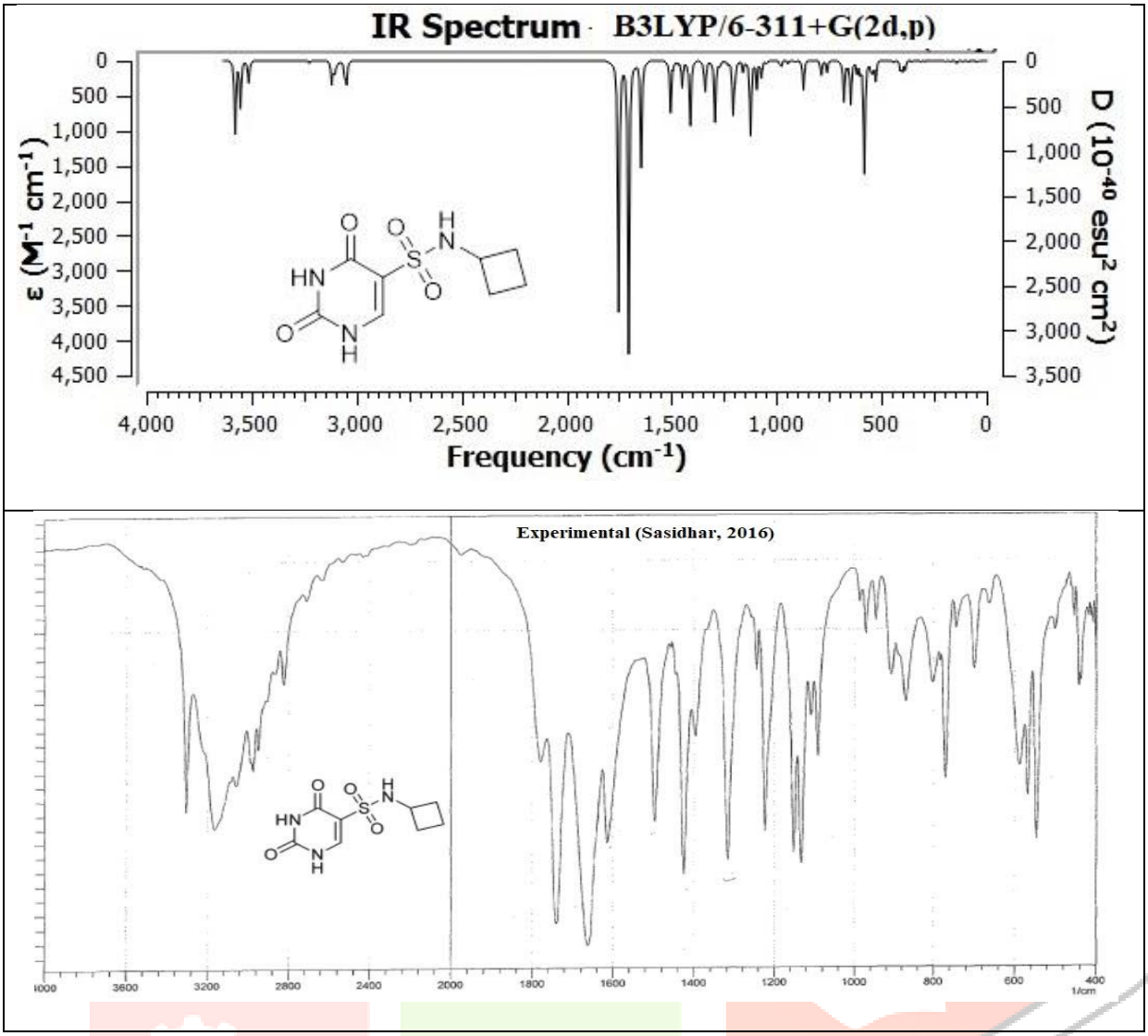

Fig. 3: Experimental and Theoretical FT-IR spectra of "N-cyclobutyl-2, 4-dioxo-1,2,3,4-tetrahydropyrimidine-5-sulfonamide"

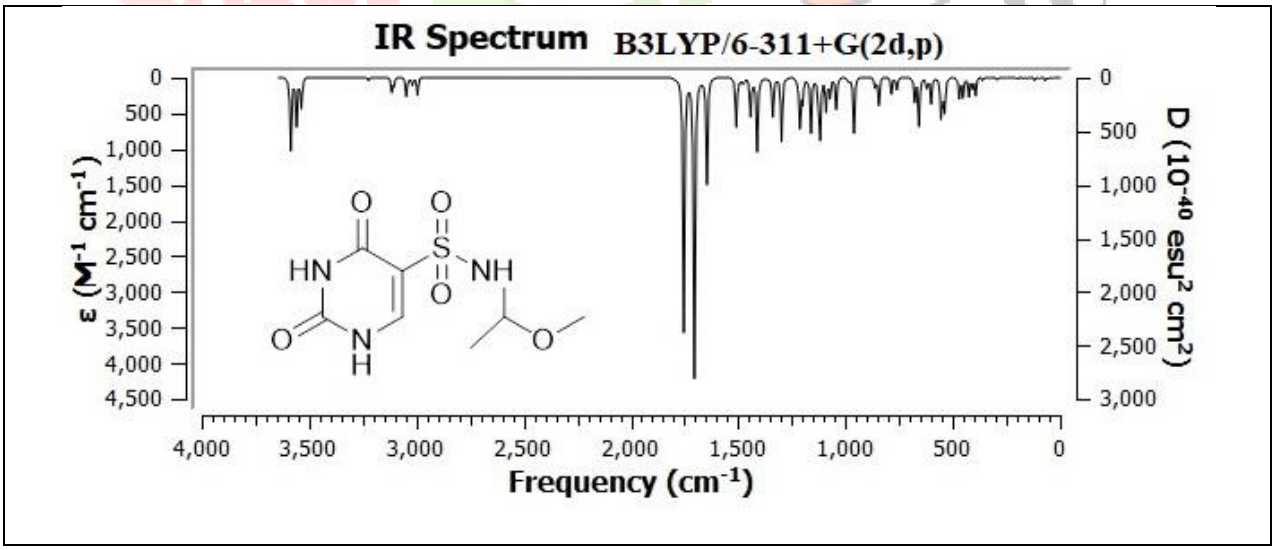

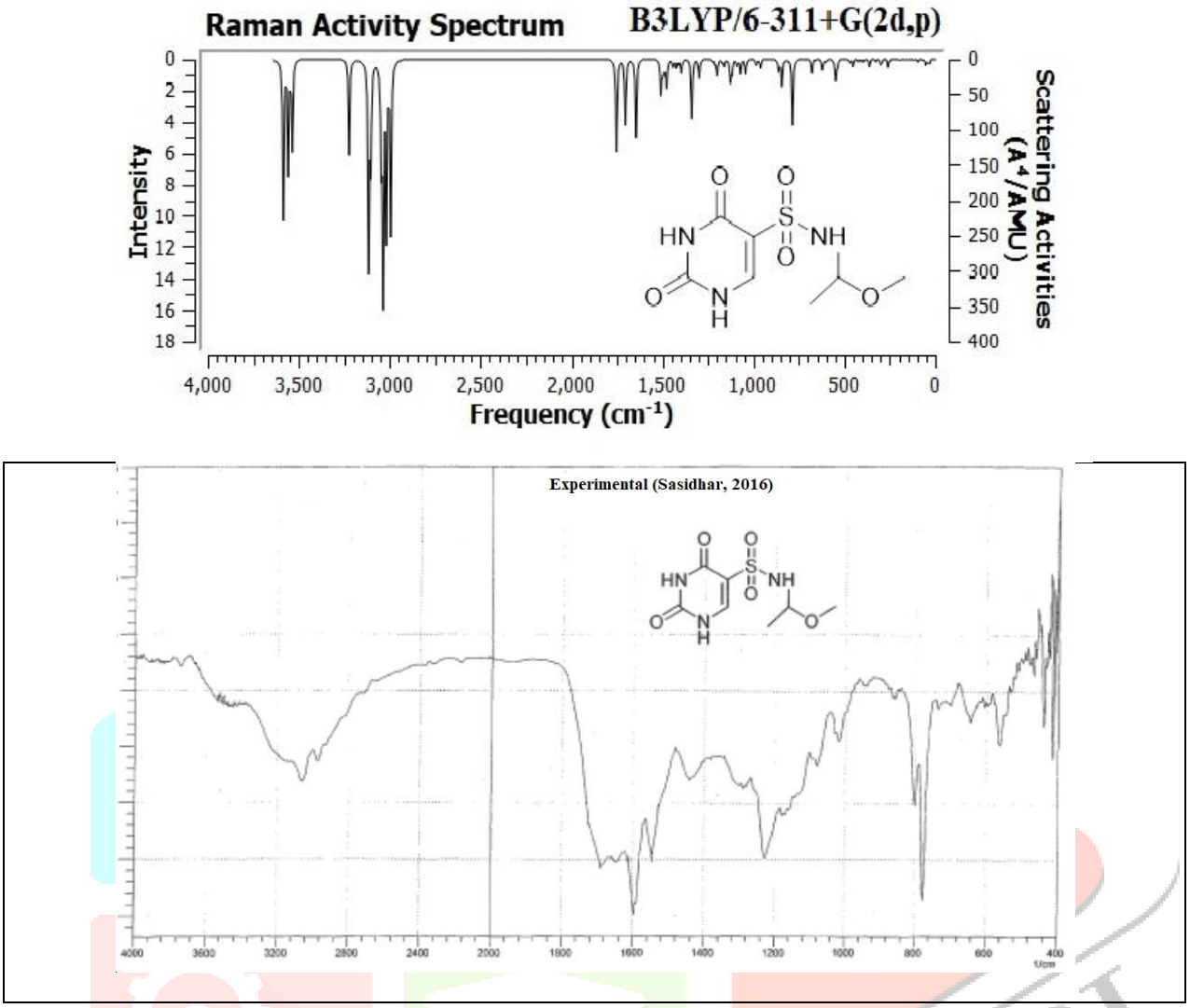

Fig. 4: Experimental and Theoretical FT-IR spectra of "N-(1-methoxyethyl)-2,4-dioxo-1,2,3,4-tetrahydropyrimidine-5-sulfonamide"

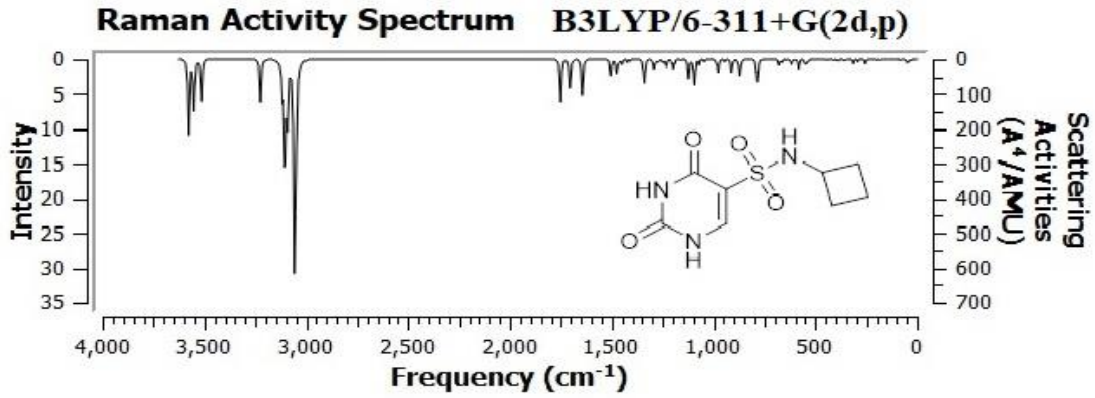

Fig. 5: Computational Raman spectra of "N-cyclobutyl-2, 4-dioxo-1,2,3,4-tetrahydropyrimidine-5-sulfonamide"

Fig 6: Computational Raman spectra of "N-(1-methoxyethyl)-2,4-dioxo-1,2,3,4-tetrahydropyrimidine-5-sulfonamide"

N-H vibrations: The usual zone for immediately detecting a hetero-aromatic structure is more than 3000 cm^{-1} for N-H stretching vibrations. Below is a list of vibrational frequencies for CH3, NH2, C=O, and C=C. The 3500–3200 cm^{-1} area is where the N–H stretching vibration happens. The scaled N-H stretch for compound 1 was calculated at 3293 cm^{-1} for the "B3LYP/6--31G(d,p)" gas phase, 3277 cm^{-1} for the "B3LYP/6--31G+(d,p)" solvent phase and "B3LYP/6--311G+(2d,p)" solvent phase, 3287 cm^{-1} for the "B3LYP/ 6--311G+(2d,p)" gas phase, and the values that were witnessed at 3250 cm^{-1} in the FT-IR spectrum. The broad spectrum of 3500–3200 cm^{-1} is where the stretching frequency occurs. For compound 2, the scaled N-H stretch has been determined at 3288cm^{-1} by the gas phase "B3LYP/6--31G(d,p)", at 3304cm^{-1} by the solvent phase "B3LYP/6-31G+(d,p)" and "B3LYP/6--311G+(2d,p)", at 3298cm^{-1} by the gas phase "B3LYP/ 6--311G+(2d,p)", and at 3330cm^{-1} in the FT-IR spectrum. The values produced conceptually using the "B3LYP/6--311+G(2d,p) and B3LYP/6--31G (d,p)" approaches exhibit outstanding concordance with the actual results of experimentation that were observed.

C-H vibrations: As the identification region for C-H stretching the frequencies, aromatic substances occur around 2800 and 3100 cm^{-1}, where C-H stretching number waves arises. For the bands that were in this position, the type of compound showed no effect. C-H stretching modes have very high Raman concentration and intensity. The C-H vibrations associated with stretching are assigned to 2910cm^{-1} in the FT-IR spectra, correspondingly. Compound 1's estimated values were calculated at 3056 cm^{-1} by "B3LYP/6-31G(d,p)"; compound 2's theoretical values were calculated at 2797 cm^{-1} by "B3LYP/6-31G(d,p)"; compound 2's hypothetical values were calculated at 2805 cm^{-1} by "B3LYP/6--31G+(d,p)"; compound 2's conceptual values were calculated at 2793 cm^{-1} by "B3LYP/6-311G+(2d,p)"; and compound 2's conceptual values were calculated at 2781 cm^{-1} by "B3LYP/ 6--311G+(2d,p)"; the results of the experiments witnessed at 2910 cm^{-1} in FT-IR spectrum method showed excellent concordance with the experimental outcomes.

C=O Vibrations: In Raman and IR, the C=O stretching vibration is seen. It is medium in the infrared at 1600 cm^{-1} and extremely faint at 1111 cm^{-1}. The calculated values of compound 1 have been found at 1678, 1695, 1651, and 1634 cm^{-1} for the gas phases "B3LYP/6-31G(d,p)", "B3LYP/6--31G+(d,p)", "B3LYP/6-311G+(2d,p)", "B3LYP/6-311G+(2d,p)", "B3LYP/6-311G+(2d,p)", and "B3LYP/ 6--311G+(2d,p)" at mode 64, and 1626, 1642, 1605, and 1589cm^{-1} for the gas phases "B3LYP/6-31G(d,p)", "B3LYP/6--31G+(d,p)", "B3LYP/6-311G+(2d,p)" and "B3LYP/ 6--311G+(2d,p)" at mode 63. These modes have experimental values of 1760 cm^{-1} and 1661 cm^{-1}, correspondingly. The calculated values of compound 2 are witnessed at 1694, 1653, 1635, and 1678cm^{-1}, accordingly, for the gas phases "B3LYP/6-31G(d,p)", "B3LYP/6--31G+(d,p)", "B3LYP/6-311G+(2d,p)", "B3LYP/6-311G+(2d,p)", "B3LYP/6-311G+(2d,p)" and "B3LYP/ 6--311G+(2d,p)" at mode 64, and 1650,1606,1590, and 1628cm^{-1}, as well, for the gas phases "B3LYP/6-31G(d,p)", "B3LYP/6--31G+(d,p)", "B3LYP/6-311G+(2d,p)" and "B3LYP/ 6--311G+(2d,p)" at mode 64. For each of these modes, the experimental values are 1640 cm^{-1}. This C=O vibration generates a

lot of free electrons, which makes this component of the molecule more bioactive when it comes to human proteins and functions as a medication.

C=C Vibrations: The spectral region of 1600–1400 cm^{-1} exhibits distinct bands in the measured FT-IR spectra due to the C=C sweet stretching vibration [11]. As a result, the C-C stretching vibrations for compound 1 that were detected in the FT-IR spectra at 1420 cm^{-1} were identified as such. Theoretically, the anharmonic frequencies at 1553cm^{-1} by the gas phase "B3LYP/6-31G(d,p)", at 1539cm^{-1} by the solvent phase "B3LYP/6--31G+(d,p)", at 1534cm^{-1} by the solvent phase "B3LYP/6-311G+(2d,p)", and at 1546cm^{-1} by the gas phase method "B3LYP/ 6--311G+(2d,p)" were assigned to the C-C stretching vibrations for compound 2, which were observed in the FT-IR spectrum at 1600cm^{-1}. The conceptually calculated anharmonic frequencies at 1560 cm^{-1} using the gas phase "B3LYP/6-31G(d,p)", at 1541 cm^{-1} by the solvent phase "B3LYP/6--31G+(d,p)", at 1535 cm^{-1} by the solvent phase "B3LYP/6-311G+(2d,p)", and at 1547 cm^{-1} by the gas phase technique "B3LYP/ 6--311G+(2d,p)" shown in excellent consistency with the results of the experiment.

3.3 NMR Assessment

NMR spectroscopy is widely used for assessing the atomic structure of organic composite materials. Chemical shifts that occur in experimental and conceptual NMR (^{1}H and ^{13}C) spectra are evaluated and expressed in Tables 4 to 7 utilizing the Gauge-Independent Atomic Orbital (GIAO) technique and Dimethyl sulfoxide (DMSO) as the standard reference. Potential NMR (^{1}H and ^{13}C) chemical shifts at the “B3LYP/ 6-311G (2d, p)” can be anticipated**.** The ^{13}C NMR spectrum displays chemical shifts for carbon atoms in the aromatic ring in the 106-143 and 104-143 ppm ranges. In the 134–143 ppm range, the carbon atoms formed a double bond with the oxygen atom [13, 14]. The aromatic ring's carbon atoms' chemical shift values were recently consistently observed to be between 113 and 159 and 100 and 164 ppm in both compounds. These ideals are supported by the investigation's findings. Double bonds between the oxygen atom and the C_2 atom are experimentally detected between 150 and 151 parts per million. There are chemical changes in the aromatic protons within the 8.02-8.20 and 8.05-8.26 ppm range. The ring structure's Uracil protons exhibit chemical shifts that are measured scientifically at 11.58 ppm, where as empirical calculations place these indications at 8.09 and 8.11 ppm. This outcome is consistent with the literature [15]. The estimated NMR (^{1}H, ^{13}C) chemical shift values accord well with the values obtained from the study.

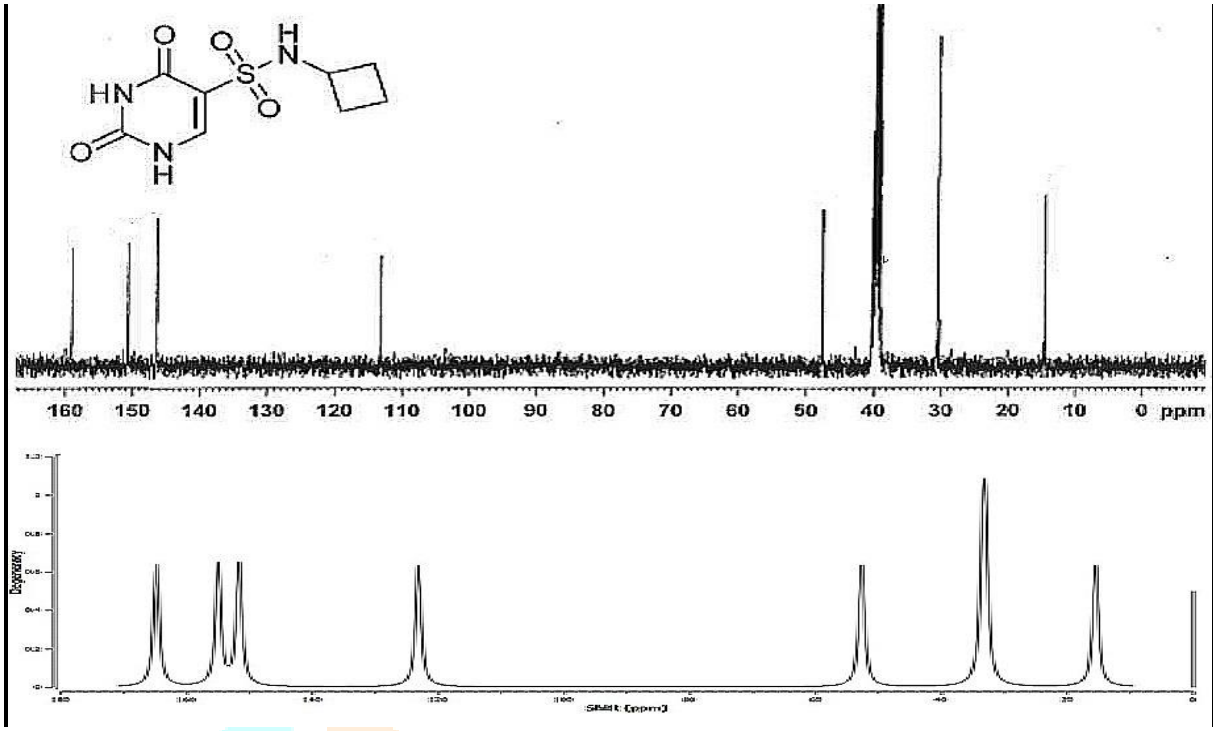

Fig. 7: Computational ^{13}CNMR spectra of 'N-cyclobutyl-2, 4-dioxo-1,2,3,4-tetrahydropyrimidine-5-sulfonamide"

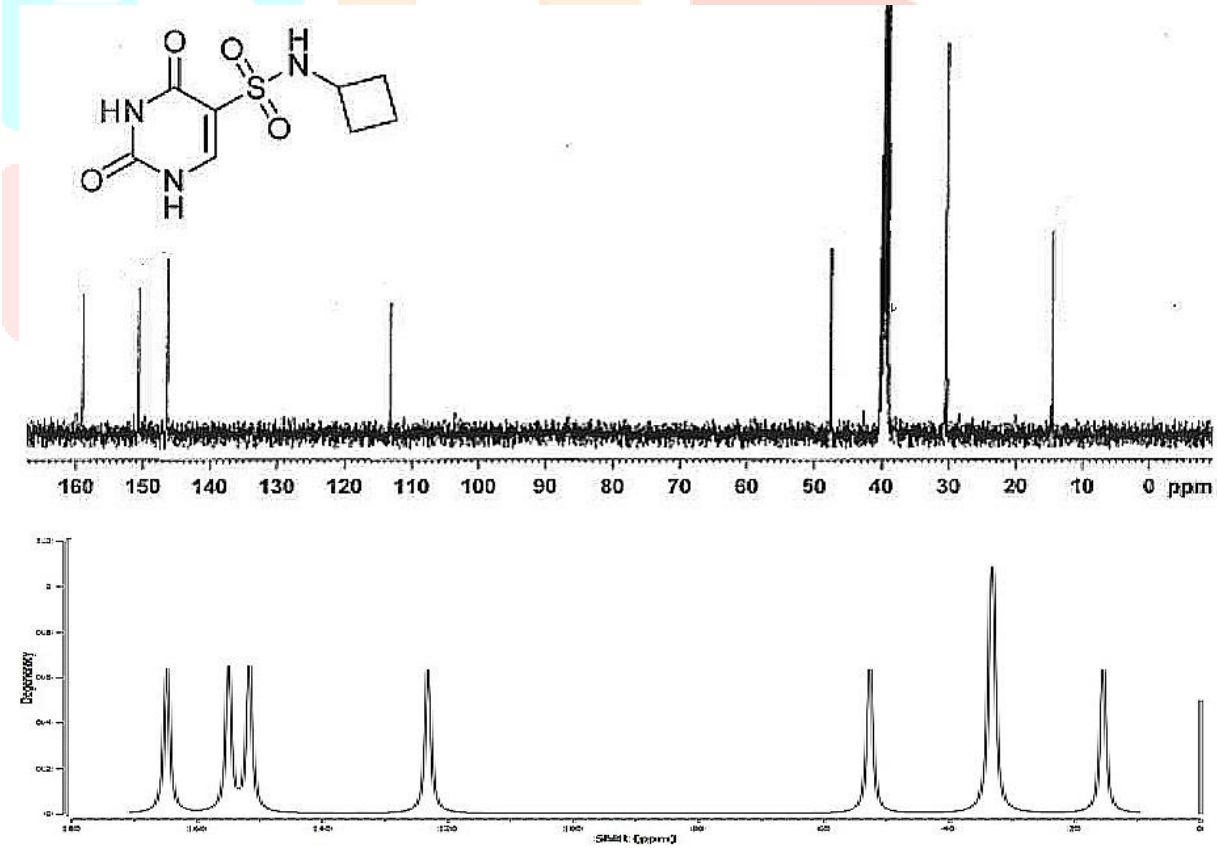

Fig. 8: Computational ^{13}CNMR spectra of "N-(1-methoxyethyl)-2,4-dioxo-1,2,3,4-tetrahydropyrimidine-5-sulfonamide"

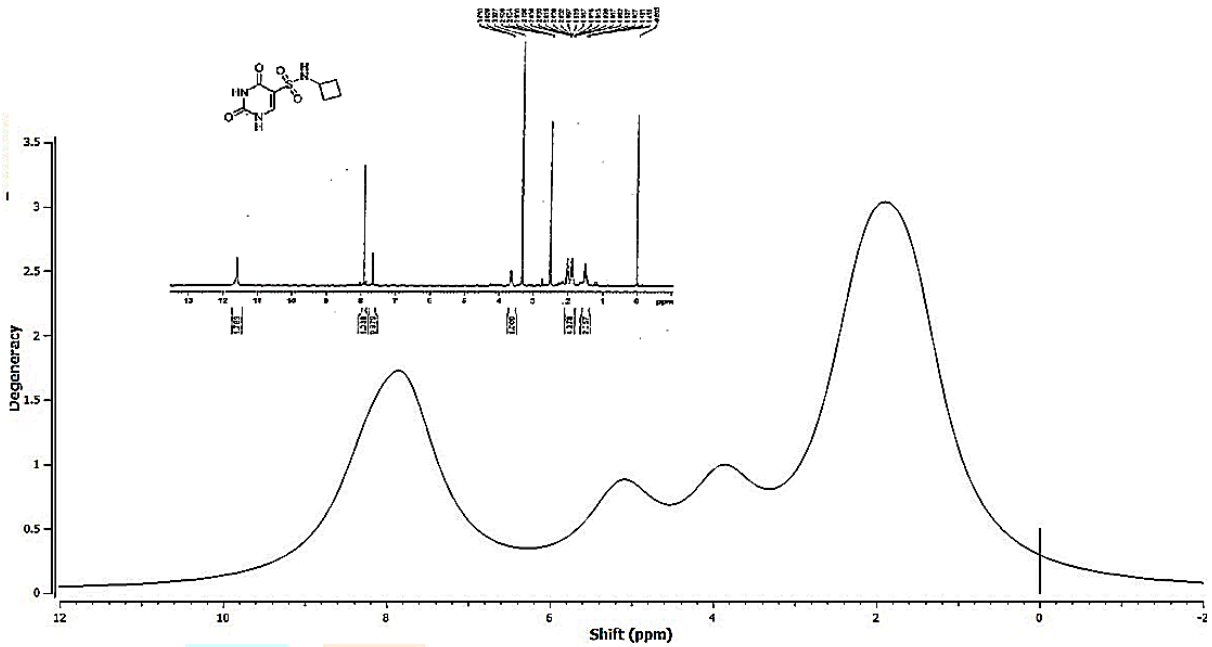

Fig. 9: Computational ^{1}H NMR spectra of "N-cyclobutyl-2, 4-dioxo-1,2,3,4-tetrahydropyrimidine-5-sulfonamide"

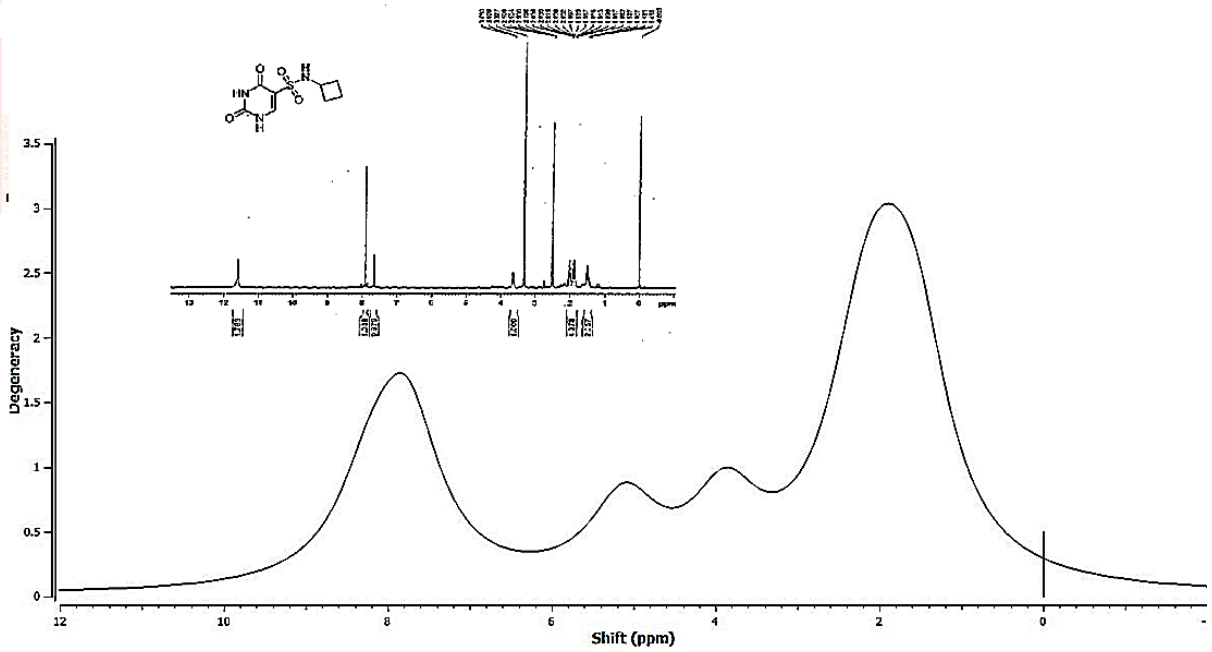

Fig. 10: Computational ^{1}H NMR spectra of "N-(1-methoxyethyl)-2,4-dioxo-1,2,3,4-tetrahydropyrimidine-5-sulfonamide"

3.4 Non Linear Optical Analysis

In modern materials science research, organic NLO materials are at the forefront. In this regard, the NLO properties of both substances were also investigated through the DFT calculations, which also included polarizability, energy, dipole moment, and first order hyperpolarizability (Parallel &

Perpendicular). For compounds 1 and 2, the characteristics such as electric dipole moment, polarizability, and first order enhanced polarizability (μ, α, Δ, and β) are calculated. NLO attributes are given in atomic units (a.u.) in Gaussian output. 1 a. u. = 8.63x10-30 esu for β, 1 a. u. = 2.54 Debye for μ, and 1 a. u. = 0.15x10-24 esu for α are used to change quantities to accepted measurements [12]. The third table provides an overview of the substances' overall static dipole moment (μ), mean polarizability (α), anisotropy of polarizability (Δ), and mean first-order hyperpolarizabilities (β). Since the urea molecule is thought to be a precursor molecule for the NLO properties, urea has been connected to the computed findings that were obtained. The urea molecule's NLO properties were computed at the same theoretical level as those of compounds 1 and 2, for comparison. The dipole moment of 2.82 D that was obtained is significantly less than the dipole moment of 3.89 D that is found in urea. In esu units, it is discovered that the two compounds' static polarizability and first order hyperpolarizability are, respectively, 21.68x10-24 to 29.78 x10-24 and 0.41x10-30 to 0.45x10-30. As a result, hyperpolarizability (βtot = 0.62x10-30 esu) is over 0.75 times greater than urea.

3.5 Analysis of UV – Visible Spectra

When analyzing the electronic spectrum of compounds using UV-vis evaluation, DFT experiments are the most common and widely used method. In this work, one electron excitation among molecular orbital is used to explain transitions from ground to excited states. In the excited state, these calculations yield the molecular geometry, absorbance maxima (max), oscillator strengths (f), and excitation energy of the molecule. Figures 11 and 12 illustrate the UV-Vis spectra predicted through the DFT approach for the basis set "B3LYP 6-311 G+ (d, p)" in DMSO solvent (SMD model).

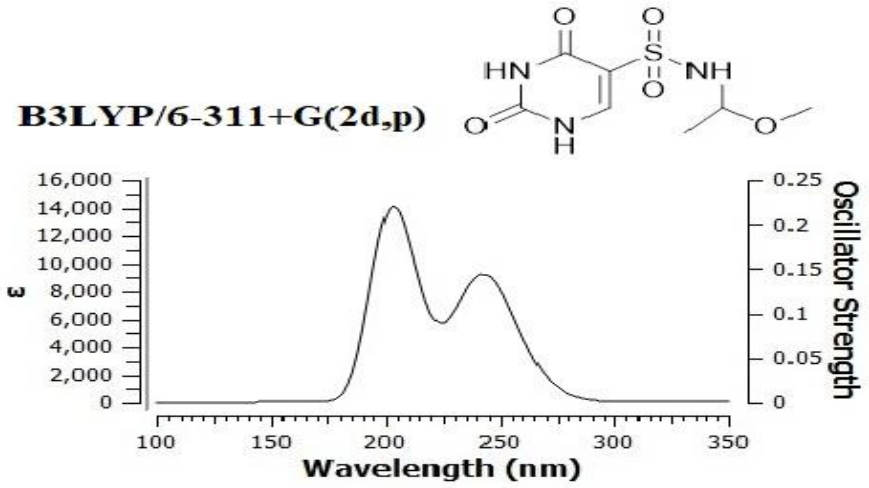

Fig. 11: Computational UV-Vis spectra of "N-cyclobutyl-2, 4-dioxo-1,2,3,4-tetrahydropyrimidine-5-sulfonamide"

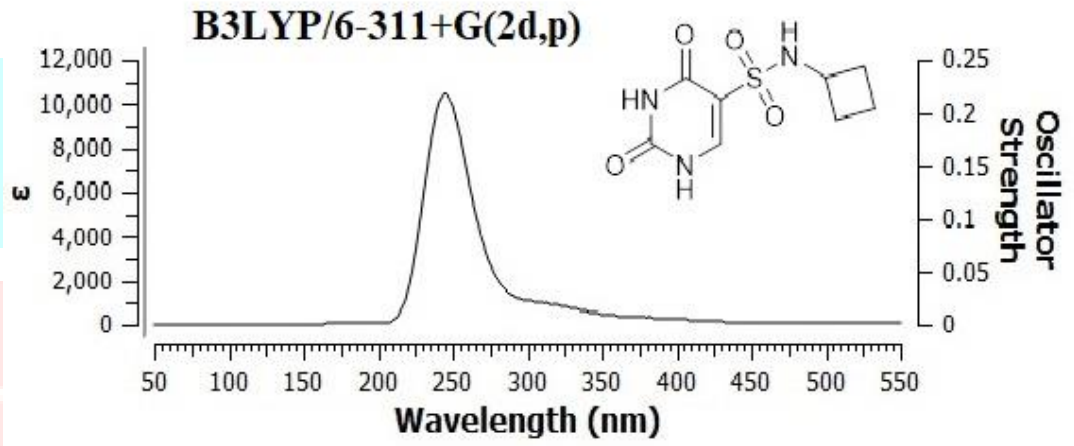

Fig. 12: Computational UV-Vis spectra of "N-(1-methoxyethyl)-2,4-dioxo-1,2,3,4-tetrahydropyrimidine-5-sulfonamide"

3.6 Frontier molecular orbital (FMO) studies

An accurate indicator of reactivity is the FMO energies and distributions. The border molecular orbitals are LUMO and HOMO. The capacity to provide an electron is shown by HOMO, while the ability to receive an electron is indicated by LUMO [17]. One of the most important indicators for assessing and defining molecule transportation characteristics is the energy gap between the HOMO and LUMO orbitals. Fig. 13 shows the 3D models of HOMO-LUMO and (H-1) - (L+1) for compounds 1 and 2. The energy gap for compound 1 is determined to be 0.190 eV, and the HOMO and LUMO energies are EHOMO = -0.275 eV and ELUMO = -0.085 eV, respectively, as shown in Fig. 14. The energies of HOMO, LUMO, and energy gap are determined to be 0.191 eV, with EHOMO = -0.277 eV and ELUMO = -0.081 eV. The energy gap is regarded as a reactivity metric, and both compounds may be thought of as extremely stable molecules because their energy gap values are less than 1 eV.

LUMO

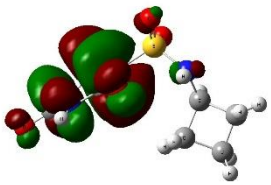

ΔE = 0.19839

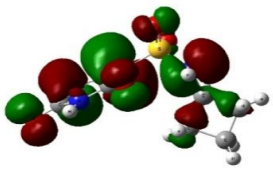

HOMO

Fig. 13: Frontier molecular orbitals of "N-cyclobutyl-2, 4-dioxo-1,2,3,4-tetrahydropyrimidine-5-sulfonamide"

LUMO

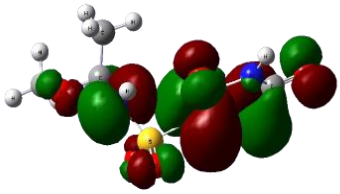

ΔE = 0.20242

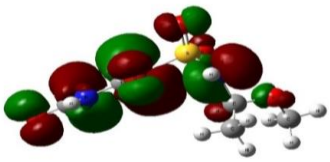

HOMO

Fig. 14: Frontier molecular orbitals of "N-(1-methoxyethyl)-2,4-dioxo-1,2,3,4-tetrahydropyrimidine-5-sulfonamide"

3.7 Drug likeness parameters

The therapeutic potential of compounds 1 and 2 has been quantified and analysed using parameters that are similar to those used in medicine. Medicine-likeness criteria are particularly helpful for the initial computation of pharmacokinetic packages, which is necessary for effective medication distribution even though they cannot anticipate whether any motes may demonstrate natural exertion. Biological characteristics like absorption (A), metabolism (M), distribution (D), toxicity (T),excretion (E), physicochemical properties, lipophilicity, pharmacokinetics, and drug similarity were computed using open source software tools like Molinspiration, pkCSM, SwissADME, and ChemAxon.

Molinspiration

Molecular modelling, drug design and miLogP (octanol/water partition coefficient) are calculated by the by the software tool molinspiration. These parameters have been calculated and are summarized in Table 8.

	N-cyclobutyl-2,4-dioxo-1,2,3,4-tetrahydropyrimidine-5-sulfonamide	N-(1-methoxyethyl)-2,4-dioxo-1,2,3,4-tetrahydropyrimidine-5-sulfonamide
miLogP	-1.02	-1.35
GPCR ligand	0.41	0.68
Ion channel modulator	0.71	0.96
Kinase inhibitor	0.84	1.01
Nuclear receptor ligand	0.78	0.94
Protease inhibitor	0.38	0.74
Enzyme inhibitor	0.11	0.26

pkCSM

Predicted pharmacokinetic properties (ADMET) calculated using "pkCSM" of molecules.

pkCSM (ADMET)	N-cyclobutyl-2,4-dioxo-1,2,3,4-tetrahydropyrimidine-5-sulfonamide	N-(1-methoxyethyl)-2,4-dioxo-1,2,3,4-tetrahydropyrimidine-5-sulfonamide
Water solubility	-3.177	-2.342
Caco2 permeability	-0.022	-0.137
Intestinal absorption (human)	61.05	44.63
BBB permeability	-0.599	-1.099
CNS permeability	-3.231	-3.305
AMES toxicity	No	No
Max. tolerated dose (human)	0.954	1.083
Oral Rat Acute Toxicity (LD50)	2.006	1.788
Oral Rat Chronic Toxicity (LOAEL)	2.082	2.416
T.Pyriformis toxicity	0.263	0.2
LogP	-1.106	-1.666

SwissADME

Predicted physicochemical properties, pharmacokinetics, Lipophilicity and drug-likeness properties using "SwissADME" web tool.

Properties	N-cyclobutyl-2,4-dioxo-1,2,3,4-tetrahydropyrimidine-5-sulfonamide	N-(1-methoxyethyl)-2,4-dioxo-1,2,3,4-tetrahydropyrimidine-5-sulfonamide
iLOGP	0.31	-0.26
XLOGP3	-0.89	-0.86
WLOGP	-0.03	-0.59
MLOGP	-0.85	-1.97
ESOL Class	Very soluble	Very soluble
Ali Class	Very soluble	Very soluble
GI absorption	High	High
log Kp (cm/s)	-8.43	-8.43
Lipinski #violations	0	0
Ghose #violations	0	1
Veber #violations	0	0
Egan #violations	0	0
Muegge #violations	0	0
Bioavailability Score	0.55	0.55

ChemAxon

Calculated logP values and other structural properties predicted using Chemaxon

Properties	N-cyclobutyl-2,4-dioxo-1,2,3,4-tetrahydropyrimidine-5-sulfonamide	N-(1-methoxyethyl)-2,4-dioxo-1,2,3,4-tetrahydropyrimidine-5-sulfonamide
Lipinski's rule of five	TRUE	TRUE
Topological polar surface area	104.37 A2	113.60 A2
Polarizability	21.72 A3	21.38 A3
logP	-1.06	-1.68
Molar refractivity	54.82 cm3/mol	53.71 cm3/mol

Quantum Computational and Spectroscopic Studies (FT-IR, FT-Raman, NMR and UV-Vis) on Uracil-5-Secondary Sulfonamides

SUPPLEMENTARY DATA

Table 1: Experimental (FT-IR) and Theoretical IR frequencies of N-cyclobutyl-2,4-dioxo-1,2,3,4-tetrahydropyrimidine-5-sulfonamide (6-311G + (2d,p) Solvent Phase).

6-311G+ (2d,p) Solvent Phase							
Mode #	Experimental	Infrared	Raman Activity	Frequency		Depolar-P	Depolar-U
				Unscaled	Scaled		
75		300.3329	309.2065	3577.36	3337.67688	0.1602	0.2762
74		190.1809	204.5917	3552.33	3314.32389	0.2107	0.3481
73	3250	89.1379	166.043	3513.26	3277.87158	0.1029	0.1866
72		10.6815	160.3412	3225.18	3009.09294	0.2842	0.4426
71		96.0943	114.9813	3118.21	2909.28993	0.2389	0.3856
70		20.1546	259.2189	3106.41	2898.28053	0.3389	0.5062
69		41.0879	226.2838	3102.2	2894.3526	0.7473	0.8554
68		12.483	206.8236	3091.3	2884.1829	0.6052	0.754
67		40.1726	666.3842	3057.56	2852.70348	0.0605	0.1141
66		39.8126	290.3214	3051.87	2847.39471	0.2197	0.3603
65	2910	81.7124	128.8725	3046.47	2842.35651	0.1375	0.2417
64	1760	1032.146	110.934	1751.68	1634.31744	0.1302	0.2305
63	1661	1205.869	74.1945	1704.05	1589.87865	0.2524	0.4031
62	1420	436.491	93.4268	1644.23	1534.06659	0.1748	0.2976
61		212.4172	38.5513	1504.72	1403.90376	0.608	0.7562
60		11.32	4.7754	1494.56	1394.42448	0.2406	0.3879
59		6.4051	32.3212	1475.77	1376.89341	0.7475	0.8555
58		5.2808	5.2906	1464.47	1366.35051	0.7291	0.8433
57		106.3606	11.6558	1449	1351.917	0.4716	0.6409
56		22.7947	7.8348	1423.46	1328.08818	0.7209	0.8378
55		265.9873	3.8048	1409.7	1315.2501	0.4564	0.6267
54		23.4811	8.1876	1345.94	1255.76202	0.476	0.645
53		118.4	53.9114	1339.37	1249.63221	0.2055	0.3409
52		251.4894	20.9739	1292.51	1205.91183	0.6807	0.81
51		9.3534	4.2386	1281.95	1196.05935	0.4842	0.6525
50		16.6256	4.6682	1271.07	1185.90831	0.4605	0.6306
49		0.3103	1.9774	1257.69	1173.42477	0.7282	0.8427
48		0.7326	6.5519	1246.32	1162.81656	0.6935	0.819
47		9.9677	15.5208	1231.47	1148.96151	0.7465	0.8549
46		213.4388	2.7082	1206.71	1125.86043	0.3205	0.4854

45		67.5828	18.6505	1197.83	1117.57539	0.5768	0.7316
44		0.2451	4.6188	1190.41	1110.65253	0.749	0.8565
43		42.3516	2.2435	1159.28	1081.60824	0.2482	0.3978
42		306.5498	42.6005	1123.44	1048.16952	0.0268	0.0521
41		111.2174	56.432	1094.26	1020.94458	0.1526	0.2649
40		67.2101	11.1492	1072.07	1000.24131	0.3152	0.4793
39		8.9215	5.0001	1046.69	976.56177	0.6965	0.8211
38		10.5347	5.1779	984.89	918.90237	0.6739	0.8052
37		4.3719	1.9005	980.44	914.75052	0.5469	0.7071
36		19.4092	26.7294	975.74	910.36542	0.0926	0.1696
35		12.4954	4.6426	946	882.618	0.6804	0.8098
34		3.0514	27.3047	913.48	852.27684	0.7365	0.8482
33		2.8394	2.3903	904.03	843.45999	0.723	0.8393
32		120.0131	34.6619	871.94	813.52002	0.1071	0.1936
31		5.9227	3.0494	791.75	738.70275	0.6229	0.7676
30		9.3829	26.4976	788.31	735.49323	0.0867	0.1595
29		47.6363	2.1526	786.43	733.73919	0.067	0.1255
28		2.3594	35.5904	783.18	730.70694	0.0523	0.0993
27		46.9209	0.0302	758.77	707.93241	0.3373	0.5044
26		165.7458	12.4269	679.39	633.87087	0.6974	0.8217
25		18.1321	6.3429	662.91	618.49503	0.1844	0.3115
24		176.2095	0.9707	646.53	603.21249	0.6867	0.8142
23		45.477	10.2118	616.62	575.30646	0.4795	0.6482
22		42.159	0.4074	601.91	561.58203	0.7488	0.8564
21		463.846	18.1076	581.53	542.56749	0.1241	0.2208
20		31.757	8.757	550.88	513.97104	0.1275	0.2262
19		38.5314	6.513	542.21	505.88193	0.2499	0.3999
18		80.5122	2.3937	528.48	493.07184	0.7457	0.8543
17		6.6723	1.9561	442.92	413.24436	0.7278	0.8425
16		37.2444	2.0941	411.02	383.48166	0.7279	0.8425
15		39.8842	2.1681	399.88	373.08804	0.628	0.7715
14		35.1795	3.3464	386.92	360.99636	0.3449	0.5129
13		5.3862	3.1699	358.07	334.07931	0.4749	0.644
12		4.8141	8.7461	313.99	292.95267	0.3152	0.4793
11		3.3996	4.5247	292.65	273.04245	0.4632	0.6331
10		0.261	8.9407	255.99	238.83867	0.215	0.3539
9		3.6453	1.7752	196.08	182.94264	0.1574	0.272

8		0.6186	1.623	182.17	169.96461	0.5712	0.7271
7		4.0066	0.0507	168.3	157.0239	0.665	0.7988
6		10.9211	0.1542	142.08	132.56064	0.5688	0.7251
5		5.4017	0.2108	112.6	105.0558	0.5466	0.7069
4		6.3782	1.9437	84.24	78.59592	0.7177	0.8357
3		7.2945	6.378	49.26	45.95958	0.7443	0.8534
2		0.9308	2.9266	37.71	35.18343	0.7497	0.8569
1		0.5206	2.4017	27.79	25.92807	0.7272	0.8421

Table 2: Experimental (FT-IR) and Theoretical IR frequencies of N-(1-methoxyethyl)-2,4-dioxo-1,2,3,4-tetrahydropyrimidine-5-sulfonamid**e** (6-311G +(2d,p) Solvent Phase).

6-311G+(2d,p)Solvent Phase							
Mode #	Experimental	Infrared	Raman Activity	Frequency		Depolar -P	Depolar -U
				Unscaled	Scaled		
75		292.4033	295.6921	3584.92	3344.73036	0.1581	0.2731
74		190.6612	205.816	3557.94	3319.55802	0.2073	0.3433
73	3100	118.8808	162.8342	3535.85	3298.94805	0.0984	0.1792
72		12.7532	162.3605	3222.98	3007.04034	0.287	0.446
71		18.7491	212.2514	3116.09	2907.31197	0.7464	0.8548
70		41.6011	154.4045	3114.14	2905.49262	0.3777	0.5483
69		30.1575	152.612	3103.99	2896.02267	0.6414	0.7815
68		74.3807	143.2297	3046.63	2842.50579	0.4986	0.6654
67		9.2194	368.6856	3036.39	2832.95187	0.0142	0.028
66		28.8955	272.1007	3018.48	2816.24184	0.1378	0.2422
65	2890	71.223	272.0769	2994.46	2793.8311	0.0228	0.0446

					8		
64	1640	1025.613	111.371	1753.34	1635.86622	0.1343	0.2368
63		1211.345	75.7448	1704.45	1590.25185	0.2449	0.3934
62	1600	426.646	90.7411	1645.55	1535.29815	0.1598	0.2756
61		197.1462	38.258	1508.92	1407.82236	0.5964	0.7472
60		12.6801	11.6155	1498.2	1397.8206	0.7437	0.853
59		7.0447	10.8027	1490.8	1390.9164	0.7494	0.8567
58		11.2358	20.4314	1477.8	1378.7874	0.7405	0.8509
57		6.7587	9.7542	1477.11	1378.14363	0.7279	0.8425
56		8.6865	2.3931	1470.01	1371.51933	0.741	0.8512
55		153.1482	7.7061	1442.26	1345.62858	0.7284	0.8429
54		13.3698	8.6439	1424.38	1328.94654	0.7281	0.8426
53		277.3374	3.4291	1411.7	1317.1161	0.4417	0.6128
52		27.7473	1.0097	1408.98	1314.57834	0.338	0.5052
51		6.8964	14.5953	1396.02	1302.48666	0.741	0.8513
50		79.0372	46.3199	1339.34	1249.60422	0.2206	0.3615
49		85.9187	18.6705	1337.98	1248.33534	0.3432	0.5111
48		256.3626	20.0852	1297.93	1210.96869	0.6865	0.8141
47		15.3141	2.0838	1222.25	1140.35925	0.3326	0.4992
46		194.8942	3.7075	1212.5	1131.2625	0.388	0.5591
45		95.3649	17.1688	1199.42	1119.05886	0.6161	0.7624
44		4.656	3.0477	1173.69	1095.0527	0.6619	0.7965

					7		
43		220.2406	6.9849	1160.62	1082.85846	0.2804	0.4379
42		80.7277	22.1398	1126.43	1050.95919	0.0454	0.0869
41		235.8638	13.527	1117.66	1042.77678	0.1385	0.2433
40		129.7855	5.9969	1090.64	1017.56712	0.173	0.295
39		76.6087	14.7442	1071.92	1000.10136	0.1486	0.2587
38		125.6847	14.6183	1043.21	973.31493	0.5156	0.6804
37		4.8	1.6189	988.98	922.71834	0.7376	0.849
36		10.9946	5.1204	983.92	917.99736	0.7309	0.8445
35		225.1243	8.7003	960.32	895.97856	0.2583	0.4106
34		38.8084	11.1526	862.47	804.68451	0.678	0.8081
33		110.9877	25.4134	844.39	787.81587	0.0486	0.0927
32		5.5251	58.4345	786	733.338	0.062	0.1168
31		59.9073	3.8839	785.78	733.13274	0.132	0.2332
30		47.6521	0.0325	760.98	709.99434	0.4863	0.6544
29		94.1921	13.1255	677.63	632.22879	0.483	0.6514
28		193.5498	0.8842	657.61	613.55013	0.7475	0.8555
27		28.0257	8.4131	622.05	580.37265	0.3958	0.5671
26		19.3821	3.2433	618	576.594	0.3399	0.5074
25		102.4653	2.3746	600.8	560.5464	0.411	0.5826
24		145.9889	2.1564	554.95	517.76835	0.5655	0.7225
23		71.8994	19.0409	547.35	510.67755	0.1129	0.2029
22		127.8159	5.4104	537.84	501.80472	0.6685	0.8013
21		81.9102	2.7745	469.74	438.26742	0.7191	0.8366
20		75.8847	6.3498	452.68	422.35044	0.096	0.1752
19		73.9583	1.7838	424.54	396.09582	0.7443	0.8534
18		38.745	1.7409	407.68	380.36544	0.5751	0.7302
17		69.561	1.8602	393.4	367.0422	0.6509	0.7885
16		10.9532	6.6052	362.45	338.16585	0.1388	0.2438
15		0.0595	1.8877	327.31	305.38023	0.6647	0.7986
14		3.2246	4.2842	299.46	279.39618	0.5045	0.6707
13		7.9247	1.5961	291.27	271.75491	0.6999	0.8235

12		0.4683	6.8234	260.4	242.9532	0.1744	0.297
11		0.2989	0.8472	246.47	229.95651	0.4353	0.6066
10		2.7318	0.2091	203.02	189.41766	0.4159	0.5875
9		4.2062	0.7802	192.36	179.47188	0.7456	0.8543
8		3.4267	0.1205	169.33	157.98489	0.6825	0.8113
7		3.5798	0.3902	152.4	142.1892	0.1515	0.2631
6		12.2002	0.7578	119.06	111.08298	0.7153	0.834
5		3.0439	2.1512	95.67	89.26011	0.724	0.8399
4		13.2743	0.8469	70.73	65.99109	0.6791	0.8089
3		4.7807	4.5348	52.89	49.34637	0.7434	0.8528
2		0.8627	2.5534	39.56	36.90948	0.7339	0.8465
1		0.5813	2.9679	30.81	28.74573	0.75	0.8571

Table 3: Electric dipole moment, polarizability and first order hyper polarizability of N-cyclobutyl-2,4-dioxo-1,2,3,4-tetrahydropyrimidine-5-sulfonamide andN-(1-methoxyethyl)-2,4-dioxo-1,2,3,4-tetrahydropyrimidine-5-sulfonamid**e** in solvent phase.

	N-cyclobutyl-2,4-dioxo-1,2,3,4-tetrahydropyrimidine-5-sulfonamide	
	a. u	esu
α_{xx}	221.725	32.8563
α_{xy}	1.32815	0.196811
α_{yy}	189.742	28.1169
α_{xz}	-35.5305	-5.26507
α_{yz}	-9.87578	-1.46344
α_{zz}	191.548	28.3844
α_0	201.005	29.7859
Δ_α	71.0884	10.5342
μ_x	0	
μ_y	0	
μ_z	2.70472	
μ	2.70472	
β_{xxx}	23.3099	0.20138
β_{yxx}	-199.26	-1.72145

	N-(1-methoxyethyl)-2,4-dioxo-1,2,3,4-tetrahydropyrimidine-5-sulfonamid**e**	
	a, u	esu
α_{xx}	206.331	30.575
α_{xy}	-0.808272	-0.119774
α_{yy}	183.399	27.1769
α_{xz}	30.0255	4.44932
α_{yz}	22.9125	3.39528
α_{zz}	189.021	28.0101
α_0	192.917	28.5873
Δ_α	68.6298	10.1699
μ_x	0	
μ_y	0	
μ_z	3.29901	
μ	3.29901	
β_{xxx}	-11.6419	-0.100577
β_{yxx}	-72.4276	-0.625718

β_{xyy}	-226.32	-1.95523	β_{xyy}	275.513	2.38022
β_{yyy}	249.33	2.15402	β_{yyy}	-38.5144	-0.332735
β_{zxx}	-169.255	-1.46223	β_{zxx}	-96.7733	-0.836046
β_{xyz}	146.957	1.26959	β_{xyz}	79.8189	0.689573
β_{zyy}	33.2782	0.287498	β_{zyy}	130.961	1.1314
β_{xzz}	88.2022	0.761999	β_{xzz}	-199.826	-1.72634
β_{yzz}	-97.6635	-0.843737	β_{yzz}	100.519	0.868408
β_{zzz}	26.8449	0.231919	β_{zzz}	-22.577	-0.195048
β_0	-65.4789	-0.565687	β_0	6.9662	0.0601825

Table 4: Experimental and Computational ^{1}H NMRdata of N-cyclobutyl-2, 4-dioxo-1,2,3,4-tetrahydropyrimidine-5-sulfonamide

Atom	**Experimental**	**Theoretical B3LYP/6-311+G(2d,p)**
Uracil NH Protons	11.58	7.77
Sulfonamide NH Proton	7.93	5.11
Uracil Ethylene Proton	7.64-7.66	8.20
Cyclobutene Protons	3.62, 3.65	3.87
Cyclobutene Protons	1.91-2.0	2.00-2.30
Cyclobutene Protons	1.45-1.52	1.53

Table 5: Experimental and Computational ^{1}H NMRdata of N-(1-Methoxyethyl)-2,4-dioxo-1,2,3,4-Tetrahydropyrimidine-5-Sulfonamide

Atom	**Experimental**	**Theoretical B3LYP/6-311+G(2d,p)**
Uracil NH protons	11.58	7.79 7.80
Sulfonamide NH proton	7.95	8.25
Ethylene and alkyl protons	4.68 2.9	4.35 3.23

Table 6: Experimental and Computational ^{13}C NMRdata of N-Cyclobutyl-2, 4-dioxo-1,2,3,4-Tetrahydropyrimidine-5-Sulfonamide

Atom	Experimental	Theoretical B3LYP/6-311+G(2d,p)
Cyclobutene Carbon	14.59	15.48
Cyclobutene two Carbons	30.61	33.01 33.42
Cyclobutene Carbon	47.60	52.67
Uracil Carbons	113.30 146.46 150.76 159.17	123.1 151.6 154.9 164.7

Table 7: Experimental and Computational ^{13}C NMRdata of N-(1-Methoxyethyl)-2,4-dioxo-1,2,3,4-Tetrahydropyrimidine-5-Sulfonamide

Atom	Experimental	Theoretical B3LYP/6-311+G(2d,p)
Alkyl Carbons	21.37 49.57 82.05	16.81 56.47 87.90
Uracil Carbons	100.35 142.37 151.28 164.48	121.60 152.02 154.89 164.56

Table 8: Molecular properties and biological activity of compound 1 and 2

	N-cyclobutyl-2,4-dioxo-1,2,3,4-tetrahydropyrimidine-5-sulfonamide	N-(1-methoxyethyl)-2,4-dioxo-1,2,3,4-tetrahydropyrimidine-5-sulfonamide
miLogP	-1.02	-1.35
TPSA	111.9	121.1
natoms	16	16
MW	245.3	249.3
nON	7	8
nOHNH	3	3
nviolations	0	0

nrotb	3	4
volume	192.2	194.8
GPCR ligand	0.41	0.68
Ion channel modulator	0.71	0.96
Kinase inhibitor	0.84	1.01
Nuclear receptor ligand	0.78	0.94
Protease inhibitor	0.38	0.74
Enzyme inhibitor	0.11	0.26

Table 9: Pharmacokinetic properties of compound 1 and 2

pkCSM (ADMET)	N-cyclobutyl-2,4-dioxo-1,2,3,4-tetrahydropyrimidine-5-sulfonamide	N-(1-methoxyethyl)-2,4-dioxo-1,2,3,4-tetrahydropyrimidine-5-sulfonamide
Water solubility	-3.177	-2.342
Caco2 permeability	-0.022	-0.137
Intestinal absorption (human)	61.05	44.63
Skin Permeability	-2.929	-2.839
P-glycoprotein substrate	No	No
P-glycoprotein I inhibitor	No	No
P-glycoprotein II inhibitor	No	No
VDss (human)	0.036	-0.474
Fraction unbound (human)	0.71	0.638
BBB permeability	-0.599	-1.099
CNS permeability	-3.231	-3.305
CYP2D6 substrate	No	No
CYP3A4 substrate	No	No
CYP1A2 inhibitior	No	No
CYP2C19 inhibitior	No	No
CYP2C9 inhibitior	No	No
CYP2D6 inhibitior	No	No
CYP3A4 inhibitior	No	No
Total Clearance	0.928	1.109
Renal OCT2 substrate	No	No
AMES toxicity	No	No
Max. tolerated dose (human)	0.954	1.083
hERG I inhibitor	No	No
hERG II inhibitor	No	No

Oral Rat Acute Toxicity (LD50)	2.006	1.788
Oral Rat Chronic Toxicity (LOAEL)	2.082	2.416
Hepatotoxicity	Yes	No
Skin Sensitisation	No	No
T.Pyriformis toxicity	0.263	0.2
Minnow toxicity	3.099	2.93
Molecular Weight	245.3	249.2
LogP	-1.106	-1.666
#Rotatable Bonds	3	4
#Acceptors	4	5
#Donors	3	3
Surface Area	90.96	90.71

Table 10: Lipophilicity and drug-likeness of compound 1 and 2 using SwissADME

Properties	N-cyclobutyl-2,4-dioxo-1,2,3,4-tetrahydropyrimidine-5-sulfonamide	N-(1-methoxyethyl)-2,4-dioxo-1,2,3,4-tetrahydropyrimidine-5-sulfonamide
Formula	C8H11N3O4S	C7H11N3O5S
Molecular Weight	245.3	249.2
#Heavy atoms	16	16
#Aromatic heavy atoms	6	6
Fraction Csp3	0.5	0.43
#Rotatable bonds	3	4
#H-bond acceptors	5	6
#H-bond donors	3	3
MR	55.89	54.28
TPSA	120.3	129.5
iLOGP	0.31	-0.26
XLOGP3	-0.89	-0.86
WLOGP	-0.03	-0.59
MLOGP	-0.85	-1.97
Silicos-IT Log P	0.43	-0.17
Consensus Log P	-0.2	-0.77
ESOL Log S	-0.88	-0.86
ESOL Solubility (mg/ml)	3.24E+01	3.46E+01

ESOL Solubility (mol/l)	1.32E-01	1.39E-01
ESOL Class	Very soluble	Very soluble
Ali Log S	-1.15	-1.38
Ali Solubility (mg/ml)	1.72E+01	1.04E+01
Ali Solubility (mol/l)	7.03E-02	4.19E-02
Ali Class	Very soluble	Very soluble
Silicos-IT LogSw	-2.33	-2.01
Silicos-IT Solubility (mg/ml)	1.15E+00	2.42E+00
Silicos-IT Solubility (mol/l)	4.69E-03	9.71E-03
Silicos-IT class	Soluble	Soluble
GI absorption	High	High
BBB permeant	No	No
Pgp substrate	No	No
CYP1A2 inhibitor	No	No
CYP2C19 inhibitor	No	No
CYP2C9 inhibitor	No	No
CYP2D6 inhibitor	No	No
CYP3A4 inhibitor	No	No
log Kp (cm/s)	-8.43	-8.43
Lipinski #violations	0	0
Ghose #violations	0	1
Veber #violations	0	0
Egan #violations	0	0
Muegge #violations	0	0
Bioavailability Score	0.55	0.55
PAINS #alerts	0	0
Brenk #alerts	0	1
Leadlikeness #violations	1	1
Synthetic Accessibility	2.54	3.14

Table 11: logP values of compound 1 and 2 using ChemAxon

Properties	N-cyclobutyl-2,4-dioxo-1,2,3,4-tetrahydropyrimidine-5-sulfonamide	N-(1-methoxyethyl)-2,4-dioxo-1,2,3,4-tetrahydropyrimidine-5-sulfonamide
Molar mass (g/mol)	245.3	249.2
Exact mass (Da)	245	249
Formula	C8H11N3O4S	C7H11N3O5S
Composition	C (39.18%)N (17.13%)O (26.09%)S (13.07%)"	C (33.73%)N (16.86%)O (32.10%)S (12.86%)"
Lipinski's rule of five	TRUE	TRUE
Van der Waals volume (A3)	193.4	197.2
Van der Waals surface area (A2)	307.2	317.1
Solvent accessible surface area (A2)	383.5	403.7
Topological polar surface area (A2)	104.4	113.6
Minimum projection area (A2)	38.47	43.25
Maximum projection area (A2)	64.26	58.96
Minimum projection radius (A)	4.21	4.52
Maximum projection radius (A)	6.2	5.4
Atom count	27	27
Heavy atom count	16	16
Asymmetric atom count	0	1
Rotatable bond count	2	3
Ring count	2	1
Aromatic ring count	1	1
Hetero ring count	1	1
FSP3	0.5	0.43
Hydrogen bond donor count	3	3
Hydrogen bond acceptor count	4	5
Formal charge	0	0
Topological polar surface area	104.37 A2	113.60 A2
Polarizability	21.72 A3	21.38 A3
logP	-1.06	-1.68
Molar refractivity	54.82 cm3/mol	53.71 cm3/mol

3.CONCLUSION

The quantum computational and spectroscopic studies on Uracil-5-secondary sulfonamides, including FT-IR, FT-Raman, NMR, and UV-Vis techniques, provide a comprehensive understanding of the molecular structure, electronic properties, and chemical behavior of these compounds.

Quantum Computational Insights: The theoretical calculations using computational methods offer valuable predictions about the molecular geometry, electronic structure, and reaction pathways of the Uracil-5-secondary sulfonamides. These studies highlight the stability of the compounds, providing insights into the influence of the sulfonamide group on the uracil base. The calculations also reveal important information about the electronic distribution and possible sites for chemical reactivity.

FT-IR and FT-Raman Spectroscopy: The vibrational spectra from FT-IR and FT-Raman provide information on the functional groups and the overall molecular structure. Key peaks corresponding to sulfonamide and uracil vibrations were identified, supporting the assignment of functional groups within the molecule. The comparison of these spectra also helps in confirming the conformational details and in distinguishing between different molecular interactions, such as hydrogen bonding, which may affect the overall stability of the compound.

NMR Spectroscopy: The NMR spectra, including both proton (^{1}H) and carbon (^{13}C) NMR, are essential for elucidating the detailed structural information of the Uracil-5-secondary sulfonamide derivatives. The chemical shifts, coupling constants, and spin-spin interactions provide insights into the electronic environment around the nuclei, helping to confirm the incorporation of the sulfonamide group and the positioning of protons and carbons in the molecule.

UV-Vis Spectroscopy: The UV-Vis spectra indicate the absorption characteristics of the compounds and the effects of the sulfonamide substitution on the electronic transitions of the uracil base. Shifts in absorption maxima compared to the parent uracil molecule can be attributed to the electronic effects of the sulfonamide group, influencing the absorption profile and potentially altering the photophysical properties of the molecule.

Overall, the combined computational and spectroscopic techniques not only validate the chemical structure of the Uracil-5-secondary sulfonamides but also provide a deeper understanding of their molecular interactions, stability, and reactivity. These insights are valuable for potential applications in medicinal chemistry, where modifications of nucleobases like uracil are explored for drug design and other therapeutic interventions.

4. ACKNOWLEDGEMENTS:

The authors are thankful to the Department of Chemistry at Sri Venkateswara University in Tirupati, India, for letting him use their labs.

5. REFERENCES:

1. Heidelberger Charles, K. Chaudhuri, peter danneberg, dorothy mooren, lois griesbach, robert duschinsky, J. Schnitzer, Pleven & j. Scheiner(1957), fluorinated pyrimidines, a new class of tumor-inhibitory compounds, nature,179, 663-666.
2. M.J. Frisch, G.W. Trucks, H.B. Schlegel, G.E. Scuseria, M.A. Robb, J.R. Cheeseman, P.M.W. Gill, B. Johnson, W. Chen, M.W. Wong, C. Gonzalez, J.A. Pople, Gaussian Inc., Wallingford, CT (2004).
3. A. Frish, A.B. Nielsen, A.J. Holder, GAUSSVIEW User Manual, Gaussian Inc., Pittsburg, PA (2001).
4. Ajmal R Bhat1*, Rajendra S Dongre2 and Pervaz A Ganie1, Petra, Osiris and Molinspiration (2018),.A Computational Bioinformatic Platform for Experimental in vitro Antibacterial Activity of Annulated Uracil Derivatives. Quarterly Journal of Iranian Chemical Communication.6,114-124.
5. S.Shefrin, Asha Asokan Manakadan, T.S.Saranya (2018), A Computational study of anticancer activity of curcumin derivatives using in silico drug designing and molecular docking tools. Asian Journal of Chemistry. 30, 1335-1339.
6. Douglas E. V. Pires, Tom L. Blundell and David B. Ascher (2015)., pkCSM: predicting small-molecule pharmacokinetic properties using graph-based signatures. J. Med. Chem. 58, 4066–4072.
7. Antoine Daina, Olivier Michielin, VincentZoete1, SwissADME: a free web tool to evaluate pharmacokinetics, druglikeness and medicinal chemistry friendliness of small molecules. Scientific reports-nature, Article number 42717(2017).
8. Arnott, J. A. & Planey, S. L. (2012), The influence of lipophilicity in drug discovery and design. Expert Opin. Drug Discov. 7, 863–875.
9. Kamel Mansouri1 , Neal F. Cariello , Alexandru Korotcov, Valery Tkachenko, Chris M. Grulke ,Catherine S. Sprankle , David Allen, Warren M. Casey, Nicole C. Kleinstreuer and Antony J. Williams (2019)..Journal of Cheminformatics.
10. Muthu, Sambanthan & Maheswari, J. (2012). Quantum mechanical study and spectroscopic (FT-IR, FT-Raman, C-13, H-1, UV) study, first order hyperpolarizability, NBO analysis, HOMO and LUMO analysis of 4-[(4-aminobenzene) sulfonyl] aniline by ab initio HF and density functional method.
11. Fritzsche, Hartmut (2010)., Vibrational spectra of benzene derivatives: Von G. Varsányi. Akadémiai Kiadó, Budapest. 1969, 430 Seiten mit zahlreichen Bildern und Tabellen.
12. H. Pir, N. Gunay, O. Tamer, D. Avcı, Y. Atalay (2013), Theoretical investigation of 5-(2-Acetoxyethyl)-6-methylpyrimidin-2,4-dione: conformational study, NBO and NLO analysis, molecular structure and NMR spectra, Spectrochim. Acta, Part A 112, 331-342.
13. L.D.S. Yadav (2005), Organic Spectroscopy, Anamaya Publishers, New Delhi, India.
14. V. Balachandran, S. Rajeswari, S. Lalitha (2012), DFT computations, vibrational spectra, monomer, dimer, NBO and NMR analyses of antifungal agent: 3,5- Dibromosalicylic acid, J. Mol. Struct. 1007, 63-73.

15. F. Bardak, C. Karaca, S. Bilgili, A. Atac, T. Mavis, A.M. Asiri, M. Karabacak, E. Kose (2016)., Conformational, electronic, and spectroscopic characterization of isophthalic acid (monomer and dimer structures) experimentally and by DFT, Spectrochim. Acta, Part A 165,33-46.
16. M. Arivazhagan , D. Anitha Rexalin (2013), Vibrational spectra, UV–vis spectral analysis and HOMO–LUMO studies of 2,4-dichloro-5-nitropyrimidine and 4-methyl-2-(methylthio)pyrimidine, Spectrochimica Acta Part A: Molecular and Biomolecular Spectroscopy, 107 , 347-358.
17. Sudhir M. Hiremath, A. Suvitha, Ninganagouda R. Patil, Chidanandayya, S. Hiremath, Seema S. Khemalapure, Subrat K. Pattanayak, Veerabhadrayya, S. Negalurmath, Kotresh Obelannavar, J. Sanja (2018)., StevanArmakovi, Armakovi, Synthesis of 5-(5-methyl-benzofuran-3-ylmethyl)-3H-[1, 3, 4] oxadiazole-2-thione and investigation of its spectroscopic, reactivity, optoelectronic and drug likeness properties by combined computational and experimental approach, Spectrochim. Acta, Part A 205, 95-110.